

FOCUSING LIMIT OF A CYCLOTRON: AXIAL BETATRON INSTABILITY AGAINST BEAM DYNAMICS APPROACH

by

Saša T. ČIRKOVIĆ¹, Jasna L. RISTIĆ-DJUROVIĆ¹,
Andjelija ILIĆ¹, Nebojša NEŠKOVIĆ¹,
Alexey S. VOROZHTSOV², and Sergey B. VOROZHTSOV²

Received on October 24, 2006; accepted in revised form on November 21, 2006

In an isochronous relativistic cyclotron, axial defocusing of a beam caused by the radial growth of the isochronous magnetic field is compensated by the azimuthal field gradient introduced by sectors. The focusing capabilities of sectors set the maximum ion energy obtainable from the machine. Usually, the focusing limit of a machine is determined by using the criterion for axial beam instability evolving from the equations of betatron oscillations. The obtained value of the focusing limit is approximate because the equations of betatron oscillations it originates from are approximate as well. The accurate value of the focusing limit is obtained by simulating accelerated beam dynamics in the extraction region. It is shown that the focusing limit of a cyclotron resulting from the two methods could differ for more than 9%. The suggested third method for focusing limit computation relies on the beam dynamics simulation along the critical equilibrium orbit rather than the acceleration orbit and thus it is less time consuming although equally accurate.

Key words: cyclotron, focusing, beam, instability, betatron oscillations

INTRODUCTION

In an isochronous cyclotron, gyration frequency of an ion is constant during acceleration. The consequential growth of the relativistic ion mass during acceleration is compensated by the appropriate radial increase of the magnetic field. Such magnetic field is referred to as the isochronous field. However, the positive radial gradient of the magnetic field causes axial defocusing of the beam. The effect is stronger for larger field gradients at large radii, *i. e.* for higher beam energies. To solve the problem, the azimuthal gradient of the magnetic field is

introduced by using additional magnetic structure elements – the sectors [1].

Figure 1 shows the detail of the magnet of the VINCY Cyclotron, the main part of the TESLA Accelerator Installation, which is under construction in the Laboratory of Physics of the VINČA Institute of Nuclear Sciences. The diameter of the magnet pole is 200 cm. The machine has four sectors per magnet pole and two dees, *i. e.*, four acceleration gaps. The azimuthal width of each sector is 42° and its spiral angle is zero. The width of each acceleration gap will be taken to be 1 cm. The extraction radius of the machine is 84 cm [2]. The bending and the focusing constants of the machine are $K_b = 135$ MeV and $K_f = 69$ MeV, respectively. Thus the limiting value of the ion specific charge $\eta = 0.51$ separates the ions whose acceleration is limited by bending characteristics from those whose extraction energy is restricted by focusing capabilities of the machine. The maximal obtainable energy of the ions whose specific charge is larger than the limiting value is set by the focusing properties. Practically, this is the H^- ion beam only. The maximal obtainable energy of all the other ion beams is determined by the bending capabilities of the machine. The focusing properties of the three model magnets of the machine

Scientific paper

UDC: 621.384.633:519.876.5

BIBLID: 1451-3994, 21 (2006), 2, pp. 40-46

Authors' addresses:

¹ VINČA Institute of Nuclear Sciences
P. O. Box 522, 11001 Belgrade
Serbia

² Joint Institute for Nuclear Research
141980 Dubna, Russia

E-mail address of corresponding author:
kosjera@vin.bg.ac.yu (S. T. Čirković)

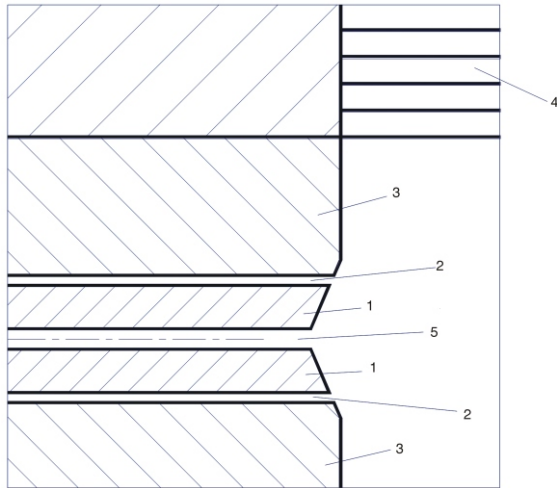


Figure 1. Detail of VINCY cyclotron magnet

The two axially opposite sectors and their surroundings in the magnetic structure: 1 – sectors, 2 – space for the trim coils, 3 – median pole plates, 4 – main coils, 5 – vertical gap between sectors i. e. magnetic gap g_m

are investigated. The models differ only by the size of the magnetic gap g_m , and the three values used are 31, 36.4, and 47.5 mm.

An isochronized magnetic field that enables isochronous regime of acceleration consists of the azimuthally averaged part, the isochronous field, and the azimuthally varying part introduced by sectors. The isochronous magnetic field is computed using Gordon's procedure [3]. The azimuthally varying part of the field is obtained and the flutter term required by Gordon's procedure is calculated from the simulated response of the model magnet. The three model magnets were created and their simulated responses obtained using MERMAID – a finite element software package for magnetic and electric field simulations [4-7]. A number of isochronized magnetic fields defined by different values of the ion gyration frequency f , was prepared for each of the three model magnets. The test ion is an H^- ion since it will be the one to be accelerated in the VINCY Cyclotron to the highest energy per nucleon.

Two of the three approaches to the focusing limit computation that will be presented rely on the concept of an equilibrium orbit. The azimuthal symmetry of the magnetic field induced by sectors is such that particles with fixed energy move on a closed trajectory called the equilibrium orbit. In a given magnetic field there is one to one correspondence between the test ion energy E , the equilibrium orbit, and the mean radius of the equilibrium orbit R_m , see fig. 2. The ion energy corresponding to the equilibrium orbit whose R_m is equal to the extraction radius of 84 cm is called the extraction energy.

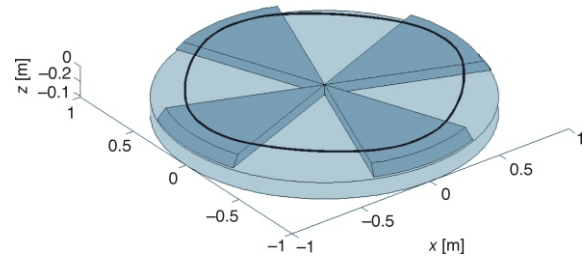


Figure 2. Equilibrium orbit

A part of the lower magnet pole, the lower sectors and an equilibrium orbit in the VINCY Cyclotron are shown. In a given magnetic field characterized by the ion gyration frequency f , an equilibrium orbit of a test ion is defined by the ion energy E , or the mean orbit radius R_m . The azimuthal half-axis $\theta = 0^\circ$ is defined by $x > 0$ and $y = 0$

AXIAL BETATRON INSTABILITY CRITERION

A test particle displaced from the equilibrium orbit oscillates around it in the radial as well as in the axial direction. These are betatron oscillations and are characterized by the radial and axial betatron frequency [8]. The focusing limit of a cyclotron results from the condition for axial beam instability which reads $\nu_z^2 = 0$, where ν_z is the axial betatron frequency. Commonly, ν_z is calculated from the following approximate expression

$$\nu_z^2 = k \frac{N^2}{N^2 - 1} F(1 - 2 \tan^2 \xi)$$

where $k = (r/\langle B \rangle)(d\langle B \rangle/dr)$ is the radial field index, r the radius, $\langle B \rangle$ the azimuthally averaged magnetic field, N the number of sectors per pole, ξ the sector spiral angle, $F = (\langle B^2 \rangle - \langle B \rangle^2) / \langle B \rangle^2$ the flutter, and $\langle B^2 \rangle$ the azimuthally averaged square of the magnetic field.

Figure 3 shows the radial dependence of ν_z^2 in the four test magnetic fields of the model magnet with $g_m = 36.4$ mm. As expected, the radial position of the axial beam instability moves towards the cyclotron centre with the increase of the gyration frequency and consequently the ion extraction energy. The minimal radius at which the instability may occur is the beam extraction radius. Thus the axial beam instability occurring at the radius of 84 cm defines the gyration frequency and magnetic field of the acceleration regime that corresponds to the focusing limit of the machine. We call this field the limiting magnetic field. In fig. 4, the radial dependence of the squared axial betatron frequency in the limiting magnetic field is given for each of the three model magnets. The focusing limit of the magnet is the energy corresponding to the equilibrium orbit with the

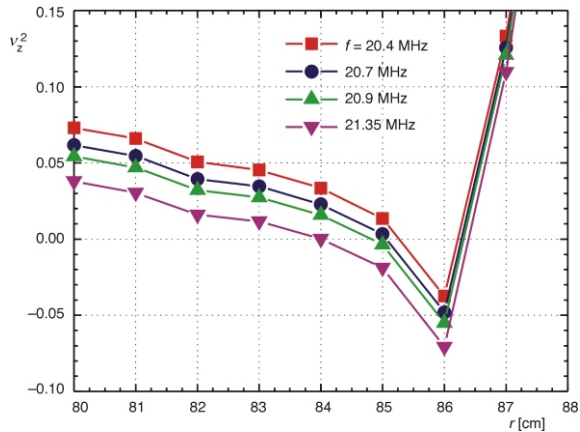


Figure 3. Radial dependence of v_z^2 in model magnet with $g_m = 36.4$ mm

The squared axial betatron frequency is shown for the isochronized magnetic fields corresponding to the four values of the ion gyration frequency $f = 20.4, 20.7, 20.9,$ and 21.35 MHz. The radial position of the axial betatron instability, $v_z^2 = 0$, decreases with the increase of the ion gyration frequency. It reaches the minimum allowed value of 84 cm, i. e., the extraction radius of the machine, for the ion gyration frequency $f = 21.35$ MHz. The isochronized magnetic field corresponding to the limiting ion gyration frequency is called the limiting magnetic field

mean radius of 84 cm in the limiting magnetic field. The obtained values of the focusing limits E_{abi} , as well as the ion gyration frequencies corresponding to the limiting magnetic fields f_{abi} , for the three cyclotron magnet models are given in tab. 1.

Table 1. Focusing limits

g_m [mm]	f_{abi} [MHz]	E_{abi} [MeV]	f_{bd} [MHz]	E_{bd} [MeV]	$\Delta E/E_{bd}$ [%]
31	22.5	84.8	21.65	77.8	9.0
36.4	21.35	75.3	20.5	68.9	9.3
47.5	19.9	64.3	19.3	60.0	7.2

The focusing limits E , and the gyration frequencies f , obtained with the axial betatron instability (abi) criterion and beam dynamics (bd) method are given for the three model magnets characterized by the magnetic gap size g_m . The focusing limits obtained using the approximate (abi) and accurate (bd) approach could differ for more than 9%

BEAM DYNAMICS METHOD

The defocusing forces are the strongest at large radii where the radial gradient of the magnetic field is the largest. Thus, the beam dynamics simulation area is chosen to be the space limited by the two equilibrium orbits with the mean radii of approximately 82 and 84 cm. The initial radial and azimuthal coordinates of the central ion in a beam are

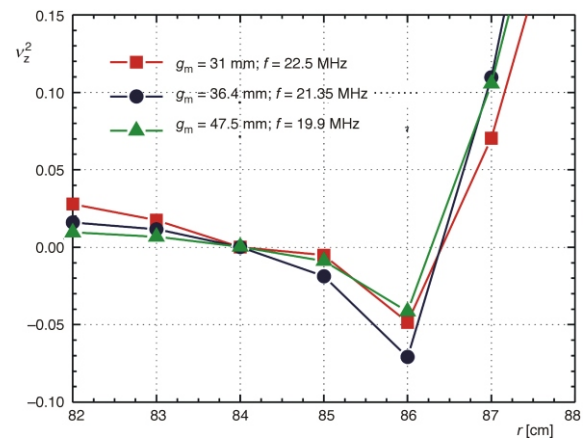


Figure 4. v_z^2 in limiting magnetic fields

The radial dependence of the squared axial betatron frequency is shown in the limiting isochronized magnetic fields of the three cyclotron magnet models. The ion gyration frequency of the limiting magnetic fields is $f_{abi} = 22.5, 21.35,$ and 19.9 MHz for the cyclotron magnet models with $g_m = 31, 36.4,$ and 47.5 mm, respectively

85 cm and 0 , respectively. At the initial point, a beam is represented by a number of ions distributed in the axial phase space. The half-axes of the initial beam emittance are 5 mm and 1 mrad. The accelerating electric field is assumed to be constant within the acceleration gap. The amplitude of the dee voltage is 70 kV. The beam simulation ends when the central ion reaches the radius of 87 cm. The output of each run is the maximum value of the axial half-envelope of the beam that was achieved during the simulation. The simulations are performed with the software package VINDY [9].

The sample beam dynamics simulation shown in fig. 5 is performed in the magnetic field corresponding to the cyclotron model with the axial gap of $g_m = 36.4$ mm and ion gyration frequency of $f = 20.9$ MHz. The maximal axial beam envelope is 26 mm which is approximately equal to $0.7 g_m$ and is 2.6 times larger than the initial vertical beam size. The growth of the beam envelope indicates that defocusing forces have overpowered the focusing forces. On the other hand, the value of v_z between radii 82 and 84 cm is in the range between 0.13 and 0.18 . These values are well above zero, which corresponds to the beam instability, and therefore do not point toward any focusing problems.

Simulations similar to the one depicted in fig. 5 are performed for a number of test magnetic fields for each of the three model magnets. The properties of an equilibrium orbit are used to describe a magnetic field by the ion extraction energy it provides. The defocusing of the beam is measured by the maximal half-envelope achieved along the simulated path. The dependences of the half-envelope's maximum on the

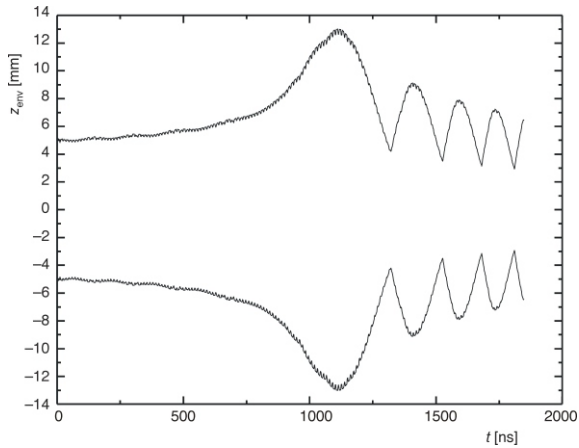


Figure 5. Axial envelope of test beam

A beam dynamics is simulated within the 2 cm wide area limited by the two equilibrium orbits. The mean radius of the outer limiting orbit is equal to the extraction radius so the simulation area is placed at the largest possible radii. Thus, in the chosen area, the beam experiences the strongest defocusing during the course of acceleration. The example corresponds to the magnet model with $g_m = 36.4$ mm and the magnetic field with $f = 20.9$ MHz. The defocusing caused by the positive radial gradient of the magnetic field emerges as the growth of the envelope in the time interval between 600 and 1000 ns from the beginning of the simulation while the focusing caused by sectors appears in the fine structure of the envelope as small dips. In general, the global maximum of the beam envelope indicates that the defocusing forces are stronger than the focusing ones. The value of the maximal half-envelope achieved along the simulated path is therefore established as a measure of the beam defocusing

extraction energy given in fig. 6 for each of the three model magnets are the results of the beam dynamics study of the focusing properties of the model magnets. The maximum of the beam envelope increases with the extraction energy increase and overgrows the size of the axial magnet gap well before the extraction energy predicted by the axial betatron instability criterion. Theoretically, any value of the maximal half-envelope of the beam that is larger than the initial half-size of the beam enlarged by the simulation error indicates the existence of the defocusing effect. The criterion used is less rigorous; namely, the focusing limit is taken to be the ion extraction energy corresponding to the value of the maximum envelope not more than 35% larger than the initial beam size which is safely above the numerical error. The focusing limits E_{bd} , as well as the ion gyration frequencies of the limiting magnetic fields f_{bd} , are listed in tab. 1.

EQUILIBRIUM ORBIT METHOD

It was shown that the beam dynamics simulations performed along the acceleration orbit in the

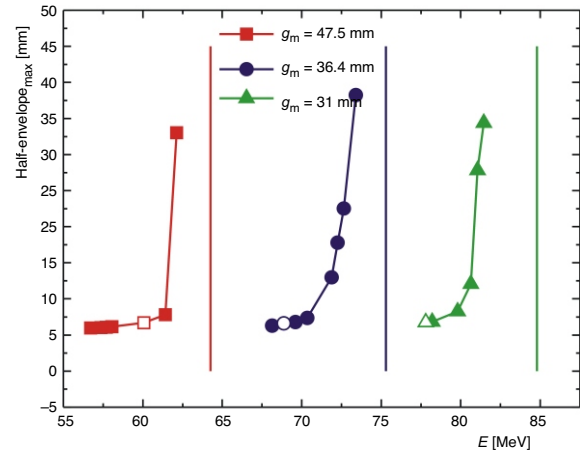


Figure 6. Maximum axial half-envelope vs. extraction energy

Each point in the graph represents a beam dynamics simulation similar to the one shown in fig. 5. The simulations differ by the isochronized magnetic field they are performed in. The magnetic fields are characterized by the ion extraction energy they provide, that is by the ion energy corresponding to the equilibrium orbit with $R_m = 84$ cm in the given field. The output of each run is the maximal axial half-envelope of the beam achieved along the simulated trajectory. The condition used to define the focusing limits is that the maximal achieved envelope is not larger than 135% of the initial vertical beam size. The points marked with an open symbol correspond to the focusing limits. The vertical lines depict the focusing limits for each of the three cyclotron models predicted by the axial betatron instability criterion

extraction region define the focusing limit more precisely than the standard axial betatron instability criterion. However, the described beam dynamics simulations are tedious because they require a very small step size and consequently substantial computational time. In our examples, the acceleration orbit makes about forty turns in the 2 cm wide simulation region. A 1 mm displacement of the simulation end point seems reasonable when compared to the radial width of the simulation area or total length of the trajectory and too large when compared to the average radial distance of 0.5 mm between the consecutive turns in the simulation area. Due to the length of the simulated trajectory, a reasonable numerical error corresponds to a large number of simulated steps. Consequently, the computational time required even for the not so large number of test particles in a beam easily overgrows the time one would be comfortable with. This problem can be solved if the simulation area is narrowed down to a single equilibrium orbit. The competition between the focusing forces of the azimuthal magnetic field gradient introduced by sectors and defocusing forces of the radial field gradient caused by the isochronous shape of the field can be observed through the axial size of the beam gyrating on an equilibrium orbit.

If the resulting forces along the orbit are defocusing, their effect is enhanced as many times as the number of turns a beam makes on the orbit. Thus, in order to detect the defocusing effect, it is sufficient to simulate only several instead of forty turns. Since the simulated trajectory is shorter, the step size providing an acceptable numerical error is larger. The shorter simulation path as well as the larger step size contributes to the smaller number of simulated steps and consequently shorter computational time. In order to enable comparison of defocusing effect at different equilibrium orbits, the criterion for the end of simulation was taken to be the fixed total length of the simulated trajectory rather than the fixed number of turns. The 30 m long simulated trajectory corresponding to approximately five to six turns and the integration step size that provides the radial simulation error equal to the one that corresponds to the accelerated orbit simulations resulted in 600 times faster simulation.

The equilibrium orbit that replaces the 2 cm wide simulation area in the beam defocusing study must be carefully chosen. It should be the orbit that is most affected by the defocusing forces. Figure 7 shows the maximal axial beam size achieved during simulation for different equilibrium orbits along which the beam gyrates in a sample magnetic field. An equilibrium orbit is characterized by its maximal orbit radius R_{\max} , rather than by its mean orbit radius R_m , to ease the justification of the orbit choice. The orbit experiencing the strongest defocusing is the one whose $R_{\max} = 86$ cm. The explanation lies in the equilibrium orbit placement relative to the maximum of the radial magnetic field gradient. On an equilibrium orbit, the beam experiences the strongest defocusing in the region where the beam trajectory is perpendicular to the radial gradient of the magnetic field. Thus, the strongest defocusing regions on an equilibrium orbit are around the maximum and the minimum orbit radii. Among equilibrium orbits in a given magnetic field, the one corresponding to the strongest defocusing has its R_{\max} in the area where the radial gradient of the field is the largest, see fig. 8. For our sample cyclotron model magnet with $g_m = 36.4$ mm the maximum of the radial magnetic field gradient is at $r = 86$ cm for all the test magnetic fields. The orbit whose minimal orbit radius is at 86 cm is not considered because it is mostly outside the isochronous field region defined by $r = 87$ cm. Therefore, the critical equilibrium orbit in a given magnetic field has its maximal orbit radius equal to the radial position of the maximum of the radial magnetic field gradient.

The curve with open symbols in fig. 9 shows the results of the beam defocusing study performed by the beam dynamics simulations along the critical equilibrium orbit. The results of the focusing limit

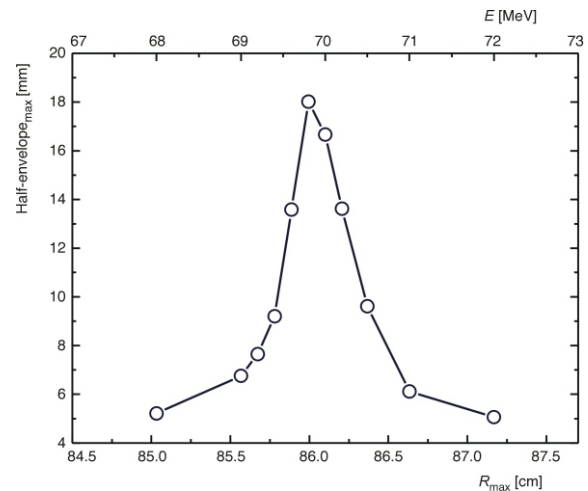


Figure 7. Beam defocusing on different equilibrium orbits

The results correspond to the model magnet with the magnetic gap of 36.4 mm and isochronized magnetic field characterized by the ion gyration frequency of 20.9 MHz. The data points on the curve represent different equilibrium orbits which are on the lower axis characterized by maximal orbit radius R_{\max} and on the upper axis by the energy of a test ion gyrating on them. A beam gyrates along each orbit until the length of the simulated trajectory reaches 30 m which corresponds to 5 to 6 turns. The dependence of the maximal obtained axial half-envelope on the equilibrium orbit along which the beam gyrates is given. The orbit corresponding to the maximum of the axial beam size is referred to as the critical equilibrium orbit. It turns out that not only for this example but also for all prepared test isochronized magnetic fields the critical equilibrium orbit has the same value of $R_{\max} = 86$ cm. Figure 8 gives the explanation of and justification for this phenomenon

study obtained with the other two methods shown in fig. 6 that correspond to $g_m = 36.4$ mm are also given in fig. 9 for the comparison purposes. The focusing limit is the point at which the slope of the curves starts to grow. Note that the “knee” of the curve corresponding to the equilibrium orbit method is more pronounced if the simulated trajectory is longer and, consequently, it is easier to determine the focusing limit. The focusing limit obtained with the equilibrium orbit method coincides with the one resulting from the beam dynamics simulation along the acceleration orbit.

CONCLUSION

The standard method to define the focusing limit of a cyclotron is to use the axial betatron instability criterion $\nu_z^2 = 0$. This equation is obtained from the simplified equations of a test particle motion around the equilibrium orbit. Since it is the instability criterion, the beam size corresponding to it is infinitely large. Therefore, the focusing limit ob-

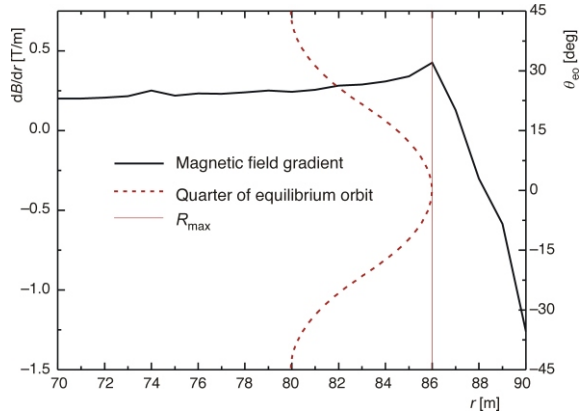


Figure 8. Critical equilibrium orbit

The radial dependence of the radial gradient of the magnetic field and a quarter of the critical equilibrium orbit is given for the model magnet with $g_m = 36.4$ mm and the isochronized magnetic field with $f = 20.9$ MHz. The defocusing axial force acting on a particle displaced from the median plane ($z = 0$) is proportional to the radial component of the magnetic field and to the azimuthal component of the particle's velocity. The azimuthal component of the particle's velocity is the largest when the radial velocity is zero, that is in the region around the maximal and the minimal equilibrium orbit radii. In the first approximation, the radial component of the magnetic field outside the median plane is proportional to the radial gradient of the magnetic field in the median plane. Thus, the strongest defocusing occurs when R_{max} is equal to the radial position of the maximal radial gradient of the field. Such equilibrium orbit is labeled as the critical equilibrium orbit

tained by using this method is not only approximate but not achievable as well. The equations of motion used to perform beam dynamics simulations along the acceleration orbit in the beam extraction region are not simplified, so this method is a more accurate method for the focusing limit computation. The criterion used to determine the value of the focusing limit is that the beam size during simulation does not increase for more than 35% which is safely above the numerical error. However, the length of the acceleration orbit in the extraction region is large, the simulation step size must be small to match the acceptable numerical error of the computation and consequently the large number of steps makes these simulations very time consuming even for the moderate number of test particles within the beam. To overcome this problem, we suggest beam dynamics simulations along the critical equilibrium orbit. The critical equilibrium orbit is the one along which the defocusing forces are pronounced mostly. It is the orbit whose maximal radius is equal to the radius of the radial magnetic field gradient maximum. The number of steps and computational time is decreased as much as 600 times with no drawbacks regarding the accuracy of the obtained focusing limit.

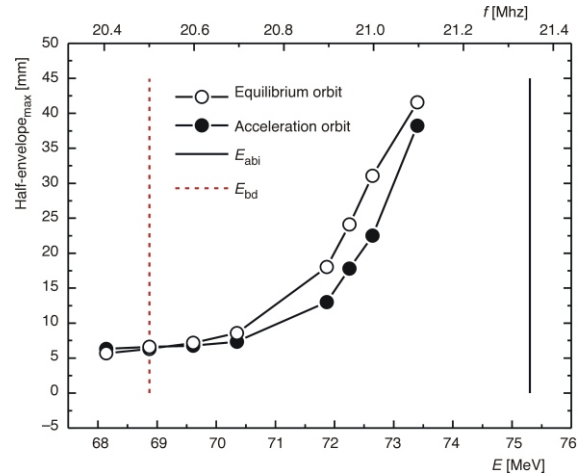


Figure 9. Focusing limits for model magnet with $g_m = 36.4$ mm

Each point marked by an open or a solid symbol represents a beam dynamics simulation performed along the critical equilibrium orbit or along the acceleration orbit, respectively. The simulations were performed in an isochronized magnetic fields defined by the ion gyration frequency and the ion extraction energy. The results represented by the solid symbols correspond to the simulations performed along the acceleration orbit and are the same as those corresponding to $g_m = 36.4$ mm in fig. 6. The solid vertical line marks the focusing limit defined by the standard axial betatron instability criterion, as in fig. 6. The criterion applied to define the focusing limit for beam dynamics simulations was that the maximal achieved beam size was not more than 35% larger than the initial beam size. The focusing limits obtained with this criterion for simulations along acceleration as well as along the critical equilibrium orbit are the same and are depicted by the vertical dashed line. Therefore, the beam dynamics simulation along the critical equilibrium orbit method for the focusing limit determination is as precise as the simulation along the acceleration orbit method but far less time consuming

REFERENCES

- [1] Livingood, J., Principles of Cyclic Particle Accelerators, Van Nostrand, Princeton, 1961, pp. 219-266
- [2] Nešković, N., Ristić-Djurović, J., Vorozhtsov, S. B., Beličev, P., Ivanenko, I. A., Ćirković, S., Vorozhtsov, A. S., Bojović, B., Dobrosavljević, A., Vujović, V., Čomor, J. J., Pajović, S. B., Status Report of the VINCY Cyclotron, *Nukleonika*, 48 (2003), suppl. 2; *Proceedings, XXXIII European Cyclotron Progress Meeting, Warsaw and Krakow, Poland, September 17-21, 2002*, pp. s135-s139
- [3] Gordon, M. M., Calculation of Isochronous Fields for Sector-Focused Cyclotrons, *Particle Accelerators*, 13 (1983), pp. 67-84
- [4] ***, SIM Limited 1994 Mermaid 2D & 3D User's Guide, Novosibirsk, Novosibirsk Department
- [5] Ćirković, S., Ristić-Djurović, J., Vorozhtsov, A. S., Vorozhtsov, S. B., Calibration of the Simulation Model of the VINCY Cyclotron Magnet, *Nuclear Technology & Radiation Protection*, 17 (2002), 1-2, pp. 13-18
- [6] Vorozhtsov, S. B., Vorozhtsov, A. S., Nešković, N., Ristić-Djurović, J., Ćirković, S., Vujović, V., Magnetic Field Simulation in the Central Region of the

- VINCY Cyclotron, *Nukleonika*, 48 (2003), suppl. 2; *Proceedings*, XXXIII European Cyclotron Progress Meeting, Warsaw and Krakow, Poland, September, 17-21, 2002, pp. 39-44
- [7] Vorozhtsov, S. B., Dobrosavljević, A., Beličev, P., Ćirković, S., Ilić, A., Košutić, Dj., Nešković, N., Rajčević, M., Ristić-Djurović, J., Vujović, V., Vukosavljević, Lj., Final Shaping of the Magnetic Structure of the VINCY Cyclotron, *Proceedings* (Eds. A. Goto, Y. Yano), 17th International Conference on Cyclotrons and Their Applications 2004, Tokyo, Japan, October 18-22, 2004, Cyclotron Center RIKEN: Particle Accelerators Society of Japan, pp. 390-392, http://tribfweb1.riken.go.jp/cyc2004/proceedings/data/CYC2004_papers/20P14.pdf
- [8] Jongen, Y., Zaremba, S., Cyclotron Magnet Calculations, *Proceedings* (Ed. S. Turner), 5th General Accelerator Physics Course, LaHulpe, Belgium, April 28 – May 5, 1994, Geneva, CERN, 1996, pp. 139-151
- [9] Ristić-Djurović, J. L., Beličev, P., Ćirković, S., Bojović, B., Nešković, N., Ion Beam Dynamics in the VINCY Cyclotron, *Proceedings* (Eds. S. Jokić *et al.*), 5th General Conference of the Balkan Physical Union, Vrnjačka Banja, Serbia and Montenegro, August 25-29, 2003 (<http://www.phy.bg.ac.yu/jdf/bpu5/proceedings>), 2003, pp. 1313-1318

**Саша Т. ЂИРКОВИЋ, Јасна Љ. РИСТИЋ-ЂУРОВИЋ
Анђелија ИЛИЋ, Небојша НЕШКОВИЋ,
Алексеј С. ВОРОЖЦОВ, Сергеј Б. ВОРОЖЦОВ**

**КОНСТАНТА ФОКУСИРАЊА ЦИКЛОТРОНА:
ОДРЕЂИВАЊЕ НАЛАЖЕЊЕМ ТАЧКЕ АКСИЈАЛНЕ БЕТАТРОНСКЕ
НЕСТАБИЛНОСТИ ИЛИ СИМУЛАЦИЈОМ ДИНАМИКЕ ЈОНСКОГ СНОПА**

У изохроном циклотрону који убрзава јоне до релативистичких енергија радијални пораст изохроног магнетског поља изазива аксијално дефокусирање снопа. Оно је компензовано утицајем азимуталног градијента поља који уносе сектори. Способност фокусирања сектора ограничава максималну енергију до које дата машина може да убрза јоне. Ова максимална енергија, тј. константа фокусирања циклотрона, обично се одређује коришћењем критеријума за аксијалну нестабилност снопа, који произилази из једначина бетатронских осцилација. Израчуната вредност константе фокусирања је приближна, јер се базира на једначинама бетатронских осцилација које су такође апроксимативне. Прецизно одређивање константе фокусирања је могуће симулацијом динамике убрзавања снопа у екстракционом региону. Показали смо да се резултати добијени применом једне, односно друге, методе израчунавања разликују чак и за више од 9%. Предлажемо коришћење треће методе одређивања константе фокусирања циклотрона, која се ослања на симулацију динамике јонског снопа дуж критичних стационарних равнотежних орбита. Предност предложеног приступа је што пружа једнаку прецизност као и метода која користи убрзане равнотежне орбите, уз значајно краће време израчунавања.

Кључне речи: циклотрон, фокусирање, снап, нестабилности, бетатронске осцилације